euspen's 22nd International Conference & Exhibition, Geneva, CH, May/June 2022
www.euspen.eu

Process behaviour of segmented and actuated tool electrodes for variable shaping in sinking EDM

Eckart Uhlmann[1,2], Kai Thißen[1], Bela Schulte Westhoff[3], Jan Streckenbach[1], Jonas Ludwig[1], Jürgen Maas[3]

[1]*Technische Universität Berlin, Institute for Machine Tools and Factuatory Management IWF, Germany*
[2]*Fraunhofer Institute for Production Systems and Design Technology IPK, Germany*
[3]*Technische Universität Berlin, Mechatronic Systems Lab EMK, Germany*

thissen@iwf.tu-berlin.de

Abstract
In sinking electrical discharge machining (S-EDM), many applications such as the manufacturing of injection moulds require numerous tool electrodes due to tool wear compensation. The manufacturing of tool electrodes causes a high cost and time expenditure in the entire process chain. This paper aims for a novel approach to a segmentation of the tool electrode in order to shape it variably. The shaping is realized by actuation of single tool electrode segments (STES) using miniaturized linear actuators. In the future, the roughing process in S-EDM could be carried out by segmenting and variably shaping of the tool electrode.
To investigate the process behaviour of a segmented tool electrode in S-EDM, different geometry configurations of the tool electrodes are compared. Experimental results show a similar material removal rate for the different tool electrode configurations. The relative linear wear of a segmented tool electrode is only 7.7 % of the relative linear wear of a monolithic tool electrode.
In order to dynamically position the STES, a miniaturized electrical linear drive is developed and constructed. The outer diameter of the actuator must not exceed the edge length of an STES. In the machine tool an actuated STES is tested and the material removal rate and the relative linear wear for different Z-axis lifting motions are analysed. The material removal rate could be increased by 37 % applying actuated Z-axis lifting motions compared to the process without Z-axis lifting motion. In this context the relative linear wear increased slightly. The results of this paper are used for the further development of the system to enable more efficient process chains in the EDM process.

Sinking electrical discharge machining, EDM, segmented tool electrode, injection mould, linear actuator

1. Introduction

Sinking electrical discharge machining (S-EDM) is a thermal process based on material removal by electrical discharges. Due to significant and non-uniform tool electrode wear ϑ, a large number of tool electrodes n is required in order to achieve the final geometry of the workpiece. This results in a high cost c and time t expenditure, since hundreds of tool electrodes have to be manufactured for a final geometry in specific machining operations. This is associated with high manufacturing time t and cost c for each workpiece [1]. In order to reduce the number of required tool electrodes n, a new approach is to divide the tool electrode into individually actuated segments, which are applied in the roughing operation in the S-EDM process. A schematic structure of the segmented tool electrode is illustrated in Figure 1. The future objective is to adaptively compose the coarse geometry of the tool electrode array using actuators, comparable to pixels in a digital image.

According to DAVE ET AL. [2], a segmentation of the tool electrode can improve the process conditions in S-EDM. In addition to that, a flushing strategy through channels in the tool electrode resulted in a higher material removal rate $\dot{V}_W$ [2]. However, the drilling of channels for active flushing involves additional cost c and time t expenditure for the manufacturing of tool electrodes. Novel flushing strategies, which will be realized by the individual actuation of the tool electrode segments, are expected to reduce the manufacturing costs c without requiring additional manufacturing efforts for the tool electrodes.

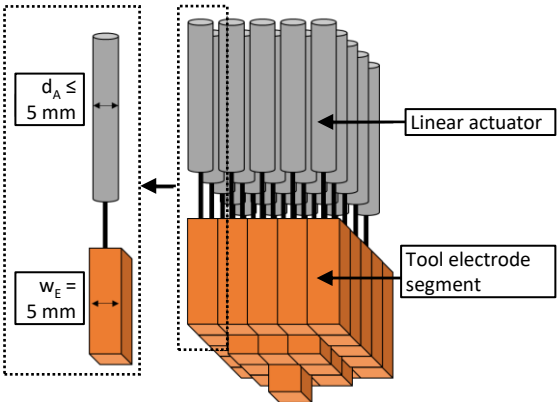

Figure 1. Bundled tool electrode assembly for S-EDM.

Besides new flushing strategies, an adaptive tool electrode geometry furthermore allows a step-by-step processing of the workpiece, which results in a reduction of the processing time t_{ero}. In section 2 of this work, the application potential of the adaptive tool electrode geometry is presented and experimentally investigated. In section 3, the material removal rate $\dot{V}_W$ and the relative linear wear ϑ_l of a single tool electrode segment (STES) with a miniaturized electrical linear drive is investigated. With the preliminary investigation of an STES in the active machine system, this work provides the basis for the future realization of the bundled geometry.

2. Subdivided S-EDM process for improved flushing

The segmentation of the tool electrode enables a subdivided S-EDM process illustrated in Figure 2, which is expected to improve the flushing conditions in the working gap s and reduce the processing time t_{ero}. The efficiency of the flushing with conventional methods decreases significantly with larger erosion depths d_e and complex geometries of the tool electrode. Due to the step geometry of the monolithic pyramid-shaped tool electrode (Figure 2a), the evacuation of debris particles out of the working gap s is more difficult.

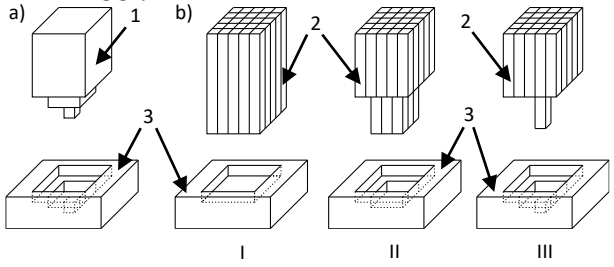

1 Solid tool electrode
2 Bundled tool electrode segments
3 Workpiece

Figure 2. Example of a pyramid geometry sunk into the workpiece. a) conventional process; b) with a segmented tool electrode.

Compared to a monolithic tool electrode, a segmented tool electrode allows a sequential S-EDM of the three cavities in the workpiece (Figure 2b). Due to the less complex geometry, an improvement for the flushing conditions is expected. To prove this hypothesis, the material removal rate $\dot{V}_W$ and the relative linear wear ϑ_l of monolithic and segmented tool electrodes are compared.

2.1. Materials and methods

In order to investigate the segmentation of the tool electrode for the roughing operation in the S-EDM process, the tool electrode material graphite EDM3, POCO GRAPHITE INC., Decatur, USA, is used. The applied workpiece material is ELMAX steel, VOESTALPINE AG, Linz, Austria. For the experiments the machine tool Genius 1000 The Cube, ZIMMER & KREIM GMBH & CO. KG, Brensbach, Germany, with the dielectric fluid Ionoplus IME-MH, OELHELD GMBH, Stuttgart, Germany, was applied.

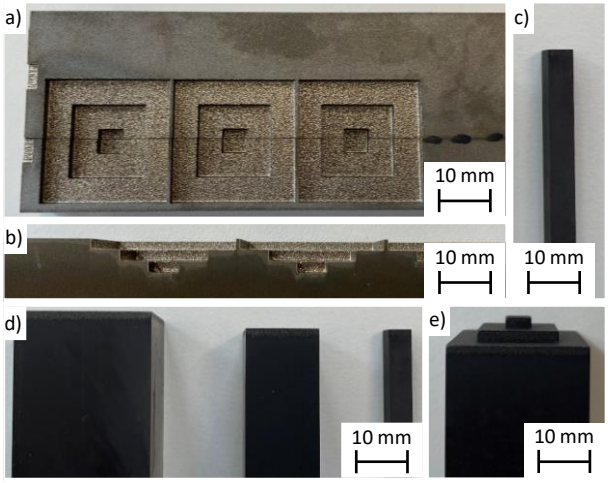

Figure 3. Workpiece cavities and tool electrode geometry configurations. a) cavity top view, b) cavity side view, c) single tool electrode segment (STES), d) monolithic tool electrode segments, e) monolithic tool electrode with pyramid structure.

In the experiments, cavities with a pyramide-like shape are machined into the workpiece, consisting of three steps, each with a erosion depth d_e = 2 mm. The cavity steps shown in Figure 3a and b have frontal surface areas of A_{E1} = 25 mm x 25 mm, A_{E2} = 15 mm x 15 mm and A_{E3} = 5 mm x 5 mm, respectively. The S-EDM is carried out with three different tool electrode geometry configurations. First, a monolithic tool electrode with pyramid structure according to Figure 3e is used. Second, the three cavity steps are manufactured sequentially with three graphite monolithic tool electrodes shown in Figure 3d. Third, the three cavity steps are also manufactured sequentially with the STES mounted statically. These STES have a square base with an edge length w_E = 5 mm. The first cavity step is manufactured with 5 x 5 STES, the second cavity step with 3 x 3 STES and the third cavity step with one STES. Each experiment is carried out three times. The applied EDM process parameters according to the guideline VDI3400 generate a surface roughness Ra = 10 µm. The material removal rate $\dot{V}_W$ is defined by the removed material volume V_W from the workpiece during the processing time t_{ero}. The removed material volume V_W is measured by the 3D-digital microscope VHX-5000, KEYENCE DEUTSCHLAND GMBH, Neu-Iseburg, Germany. The relative linear wear ϑ_l is calculated by measurements of the respective STES at a reference point on the workpiece before and after the S-EDM process.

2.2. Process behavior of segmented graphite tool electrodes

The material removal rate $\dot{V}_W$ and the relative linear wear ϑ_l, which was measured on the top of the pyramid structure, with the respective standard deviations are shown in Figure 4.

The highest material removal rate occurs with the STES at $\dot{V}_W$ = 45.90 mm³/min. The material removal rate for the three monolithic tool electrode segments is $\dot{V}_W$ = 45.83 mm³/min and the lowest material removal rate occurs for the monolithic tool electrode with pyramid structure with $\dot{V}_W$ = 45.38 mm³/min. However, the relatively small deviations between the material removal rates $\dot{V}_W$ are in the range of the standard deviations of the experiments.

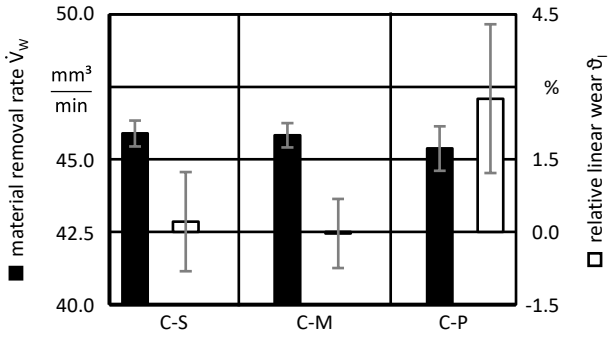

Figure 4. Material removal rate $\dot{V}_W$ and relative linear wear ϑ_l with different tool electrode configurations (C-S: single tool electrode segments, C-M: monolithic tool electrode segments, C-P: monolithic tool electrode with pyramid structure).

The relative linear wear for the STES is ϑ_l = 0.21 %. The lowest relative linear wear occurs when applying three monolithic tool electrode segments with ϑ_l = -0.03 % and the highest relative linear wear occurs for the monolithic tool electrode with pyramid structure with ϑ_l = 2.76 %. Due to the subdivided sinking process the relative linear wear ϑ_l at the top of the segmented tool electrodes is lower than the relative linear wear ϑ_l at the top of monolithic tool electrode with pyramid structure. The reduced thermal stress on the top of the tool electrode, due to less process interaction, can be seen as a significant advantage compared to conventional processing with a single monolithic tool electrode. A negative relative linear wear can occur through deposits of workpiece material on the tool electrode [5].

3. Realization of a single actuated tool electrode segment

3.1. Miniaturised electric linear drive

The objective of the developed linear drives is to dynamically generate different shapes of the tool electrode geometry. Furthermore, the actuators are utilized to generate oscillating wave movements for a novel transverse wave flushing strategy in the dielectric fluid. To meet these requirements, the developed linear drive must provide a static working lifting motion of s_w = 30 mm with a stationary positioning accuracy of $a_{SP} \leq 10$ µm and a dynamic excitation at a slider-amplitude A ≈ 1 mm as well as a frequency up to ω ≤ 10 Hz. Application-related, the installation space is severely limited, requiring the actuator to have an outer diameter d_A = 5 mm, see Figure 1 and [3]. The designed miniaturized linear drive is shown in Figure 5. A two-phase linear actuator was developed to meet both the transient performance and the space constraints of the actuator. The detailed design, modelling and control of the miniaturized linear drive is presented in [4].

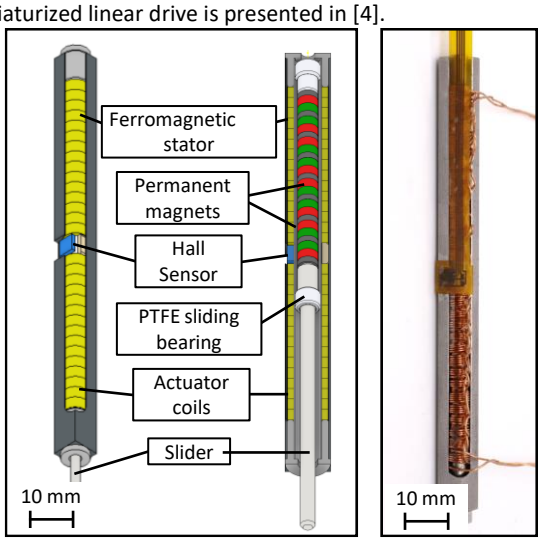

Figure 5. Design drawing and picture of the miniaturized electric linear drive.

In order to detect the position of the slider during the EDM process, a Hall sensor is implemented in the actuator. The sensor detects the position-dependent magnetic field of the permanent magnets enclosed in the slider, with this data the slider position of the actuator can be determined. The position detection of the Hall sensor for a section of the slider lifting motion is displayed in Figure 6, where it is compared with the measurement by a laser sensor. Results of the position detection show negligible deviations between the Hall sensor and the laser sensor.

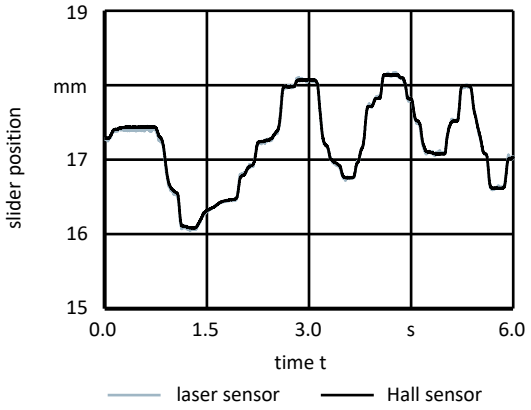

Figure 6. Measurement of the slider position comparing results of Hall sensor and laser sensor.

Figure 7 shows the deviation of the position detection by the Hall sensor compared to the laser sensor. Approximating the deviation by a normal distribution yields in a standard deviation of σ = 17.6 µm.

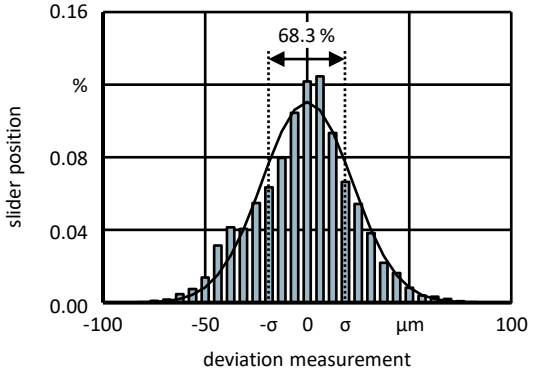

Figure 7. Deviation of the position detection by the Hall sensor compared to the laser sensor.

3.2 Implementation of a single actuated tool electrode segment in the S-EDM process

The implementation of the miniaturized linear drive in the Genius 1000 machine tool is illustrated in Figure 8. An insulating coupling is used to attach the electrode rod to the slider of the linear actuator. The actuator is clamped into the machine system using a 3D-printed mounting bracket.

Using a single actuated electrode rod, it is not yet possible to realize a discretized transverse wave flushing strategy. However, the flushing performance of an STES can be investigated experimentally.

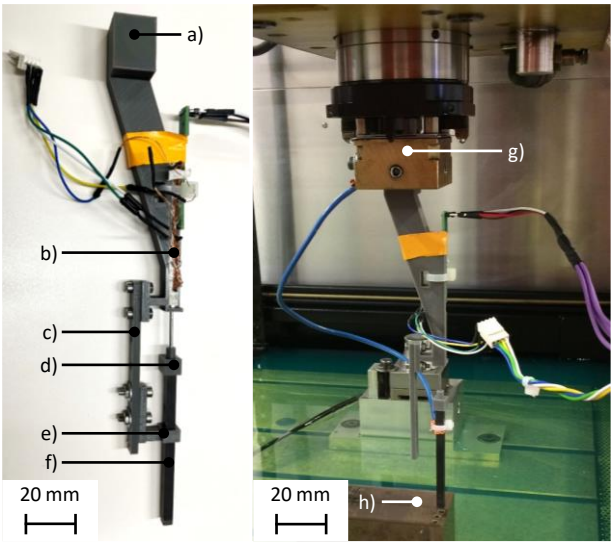

Figure 8. Combination of the linear actuator with an STES by the 3D printed bracket. a) clamping for the actuated STES, b) linear actuator, c) guide bar, d) coupling between actuator rotor and STES, e) guide rail for the STES, f) STES, g) tool electrode holder, h) workpiece.

The actuator keeps the STES in processing distance d_{ero} to the workpiece electrode for a time period T_e = 0.7 s and subsequently realizes one harmonic flushing period for a flushing time T_f = 0.1 s with an amplitude A_f = 2 mm to remove debris particles from the working gap s.

Figure 9 displays both the targeted and the actual process lifting motion of the linear actuator. The position measurement during the flushing period reveals that the system has non-modeled nonlinearities, resulting in deviations between setpoint and actual value of the position. These nonlinearities are due to position and speed dependent friction forces F_f acting on the slider. In future work, the friction forces F_f exerted on the slider will be investigated in more detail to compensate the nonlinear

behaviour and consequently improve the dynamic position control.

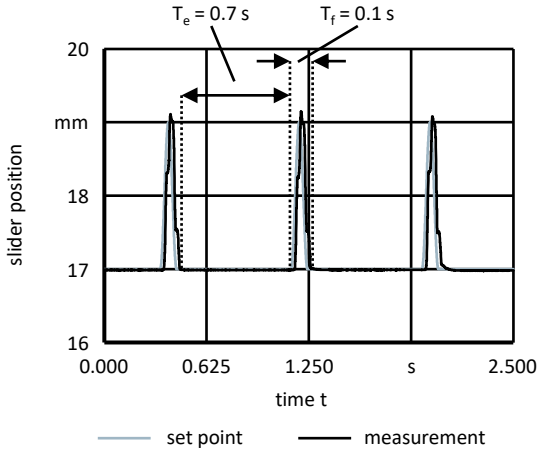

Figure 9. Position set point and measurement data of the actuated Z-axis lifting motions.

3.3. Experimental validation

To analyse the process behaviour of an actuated STES, experiments are carried out with different Z-axis lifting motions. The material removal rate $\dot{V}_W$ and the relative linear wear ϑ_l are compared without Z-axis lifting motions, with Z-axis lifting motions by the machine tool and with Z-axis lifting motions performed by the actuator. Shielded cables are used to reduce electromagnetic interference from actuators and sensors.

Figure 10 shows the material removal rate $\dot{V}_W$ and the relative linear wear ϑ_l of the experiments. The material removal rate without a Z-axis lifting motion is $\dot{V}_W$ = 4.10 mm³/min with a relative linear wear ϑ_l = 2.24 %. With a Z-axis lifting motion by the machine tool the material removal rate $\dot{V}_W$ = 6.45 mm³/min is the highest with also the highest relative linear wear ϑ_l = 4.60 %. The Z-axis lifting motion by the actuator generates a material removal rate $\dot{V}_W$ = 5.64 mm³/min and a relative linear wear ϑ_l = 2.31 %. Thanks to the Z-axis lifting motion by the actuator, a significantly higher material removal rate $\dot{V}_W$ by 37 % with only slightly higher relative linear wear ϑ_l can be achieved compared to the experiments without a Z-axis lifting motion. It is assumed that this improvement is a consequence of better flushing conditions in the working gap s. It has to be admitted that processing without Z-axis lifting motions is disadvantageous for the processing conditions due to a total lack of flushing and not state of the art.

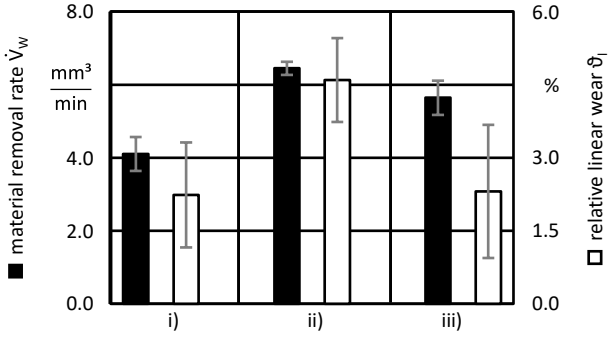

i) without Z-axis lifting motion

ii) Z-axis lifting motion by the machine tool

iii) Z-axis lifting motion by the actuator

Figure 10. Material removal rate $\dot{V}_W$ and relative linear wear ϑ_l for different Z-axis lifting motions.

The application of the actuator did not lead to an improvement of the material removal rate $\dot{V}_W$ compared to the Z-axis lifting motion by the machine tool. However, the relative linear wear ϑ_l could be halved by the Z-axis lifting motions applying the actuator compared to the Z-axis lifting motions by the machine tool. As shown in Figure 10, the material removal rate $\dot{V}_W$ of the Z-axis lifting motion by the machine tool is higher than for the Z-axis lifting motion by the actuator. This could be attributed to the machine feed control system, which is counteracting the lifting motion of the actuator.

4. Conclusions and outlook

In this paper, the process behavior of segmented tool electrodes in S-EDM was investigated. These tool electrodes can form variable shapes for the roughing operation in S-EDM via linear actuation of the STES. This approach can save costs c and material for the manufacturing of the tool electrodes in the future, since the roughing can be carried out by the variably formable tool electrode. This approach could save the use of numerous tool electrodes in the roughing operation.

In the experiments the material removal rate $\dot{V}_W$ and the relative linear wear ϑ_l of a segmented tool electrode were analysed and compared to a monolithic tool electrode. The results show a similar material removal rate for the different tool electrode configurations. The relative linear wear at the top of the segmented tool electrode C-S is only 7.7 % of the relative linear wear of a monolithic tool electrode with pyramid structure C-P. For the actuation of the STES the outer limitations of the linear actuator must not exceed the chosen edge length of an STES with w_E = 5 mm. A miniaturized electrical actuator was developed for this purpose. The coupling of the actuator and a STES was implemented in the machine tool with the use of 3D-printed components. Experiments with Z-axis lifting motions by the actuator show a significantly higher material removal rate $\dot{V}_W$ with only a slightly higher relative linear wear ϑ_l compared to tests without Z-axis lifting motions. This work showed the applicability of an actuated STES in the EDM process and the possibility of process optimization by further research.

In future work, several actuated STES will be combined to form an actuated tool electrode module consisting of 3 to 5 individual segments. With this system, a new type of flushing strategy will be investigated in the EDM process, which generates transverse waves through peristaltic movements of the STES. The processing time t_{ero} can be shortened by a more effective flushing and thus the production costs c can be reduced.

Acknowledgements

The authors thank the Deutsche Forschungsgemeinschaft e.V. (DFG) for funding this project.

References

[1] Uhlmann E, Mullany B, Biermann D, Rajurkar K P, Hausotte T and Brinksmeier E 2016 Process chains for high-precision components with micro-scale features *CIRP Annals* **65** 549 - 572

[2] Dave H K, Kumar S, Rana N C and Raval H K 2014 Electro discharge machining of AISI 304 using solid and bundled electrodes *Proceedings of the* **26***th AIMTDR* 296-1 - 296-7

[3] E. Uhlmann et al.: Concept for an actuated variable tool electrode for use in sinking EDM, Proceedings of the **21**st conference of the euspen, 183-184, 2021

[4] Schulte Westhoff B and Maas J 2021 Modeling and Control of Miniaturized Electric Linear Drive with Two-phase Current Excitation *IEEE/ASME International Conference on Advanced Intelligent Mechatronics (AIM)* 332-337

[5] Klocke F, Schwade M, Klink A and Veselovac D 2013 Analysis of material removal rate and electrode wear in sinking EDM roughing strategies using different graphite grades *Procedia CIRP* **6** 163-167